

# Chemiluminescent pathways in reactions of phosphorus, antimony, and bismuth with ozone to form dioxides and monoxides

Rodger P. Kampf and John M. Parson

Department of Chemistry, The Ohio State University, Columbus, OH 43210

(Received 5 December 1997; accepted 2 February 1998)

Chemiluminescent (CL) reactions have been observed using molecular beams of phosphorus, antimony, and bismuth colliding with ozone as a scattering gas. The fluorescence spectra indicate the formation of electronically excited  $\text{PO}_2$ ,  $\text{SbO}_2$ , and  $\text{BiO}_2$ , and probably  $\text{SbO}$  and  $\text{BiO}$ , as well. None of the emitting states of the dioxides seem to correspond to previously characterized states. Since the beam source could generate variable ratios of atoms, dimers, and tetramers, the CL reactions can be attributed to P, Sb,  $\text{Sb}_2$ , and Bi. The assignments of reactant species were aided by measurements of the total CL dependence on the beam time dependence. The time-dependent experiments also revealed CL reactions of antimony and bismuth, which are second order in ozone. Fits to the time-dependent spectra show that whereas the first-order CL reaction of P proceeds without a potential barrier, for  $\text{Sb}_n$  and Bi, only the second-order CL reactions can occur without very high barriers. © 1998 American Institute of Physics. [S0021-9606(98)00718-1]

## INTRODUCTION

The kinetics and spectroscopy of heavier group VA dioxides are not well known. Some of these dioxides have not previously been definitively identified in the gas phase, although the monoxides have. Despite a rather complex spectroscopy arising from closely spaced and perturbing electronic states, many of the lower-lying states of  $\text{NO}_2$  have been characterized.<sup>1-12</sup> Gradually, a better understanding of these states has emerged. Some constants are known for the  $\text{PO}_2$  ground state,  $\tilde{X}^2A_1$ , and for some low-lying electronic states, including  $^2B_2$  and  $^2B_1$  states, which may have been observed by previous investigators; see Table I. There is still, however, some confusion as to the identity of emitting states of  $\text{PO}_2$ . And for Sb and Bi, the dioxides have not been definitively identified and, as of yet, no constants are available.

Understanding the nature of the low lying excited states of  $\text{NO}_2$  may help assign low-lying electronic states of  $\text{PO}_2$  and other members of this group. The vibrational frequencies and geometry of the ground state of  $\text{NO}_2$  have been fairly well determined, but perturbations are especially prevalent in the  $\tilde{A}^2B_2$  state (which correlates to  $^2A'$  in  $C_s$  symmetry). The perturbations are believed to arise from mixing with high-lying vibrational states of the ground electronic state. For the three lowest electronically excited states Gillispie and co-workers<sup>13</sup> have provided geometries and vibrational constants for the symmetric stretch and bending modes through *ab initio* calculations. These constants may be considered to be fairly good estimates to the actual values, as there is good agreement of ground state results with experimental values.<sup>6,10</sup>

A further complication is that the  $\tilde{A}$  state's two N-O bond lengths are most likely unequal.<sup>14-19</sup> The molecule in this electronic state would then belong to the  $C_s$  point group and the state would more properly be designated  $^2A'$ . Relatively recent experimental investigations,<sup>10,11</sup> though, have provided more detailed spectroscopic information concern-

ing the  $\tilde{A}$  state, including an accurate value of the excitation energy  $T_0$ . While the issue of the equality of the two N-O bonds was not discussed in these experimental investigations, the most recent *ab initio* calculations by Buenker and co-workers<sup>17</sup> suggest only a small deviation from equality in the two N-O bond lengths.

Spectroscopic information on  $\text{PO}_2$  has been obtained from a variety of methods. See Table I. Verma and McCarthy<sup>20</sup> observed  $\text{PO}_2$  in a flash discharge experiment, and although their bending mode assignments were apparently incorrect, they have established an electronic origin,  $T_0$ , of about  $30\,380\text{ cm}^{-1}$ . The ground state vibrational frequencies and geometry have been reasonably well determined from infrared laser magnetic resonance (LMR)<sup>21</sup> and through laser-induced fluorescence (LIF) studies by Hamilton.<sup>22,23</sup> Stedman and co-workers,<sup>24,25</sup> as well as Cool and co-workers,<sup>26</sup> have observed chemiluminescence (CL) from reactions of phosphorus with  $\text{O}_3$  and other oxidizing environments forming  $\text{PO}_2$  under multiple-collision conditions. Lohr has performed *ab initio* calculations<sup>27</sup> for a low-lying  $^2B_1$  electronic state, which, similarly to  $\text{NO}_2$ , has been found to be a linear  $^2\Pi_u$  state. More recent *ab initio* calculations by Buenker and co-workers<sup>28</sup> and Kabbadj and Leivin<sup>29</sup> have also approximated the locations of low-lying  $^2A_2$  and  $^2B_2$  states, as well as higher states. Andrews and co-workers<sup>30-33</sup> have conducted a series of investigations on the spectra of products from reactions of phosphorus containing compounds with  $\text{O}_3$ , trapped in argon matrices, with products including  $\text{PO}_2$ .

Both Stedman and Hamilton seem possibly to have observed two electronic states in their investigations. Hamilton detected different radiative lifetimes in different parts of the LIF spectrum. He has argued that, similarly to  $\text{NO}_2$ , high-lying vibrational levels of the ground electronic state may perturb some of the linear  $^2B_1$  upper state vibrational levels, changing the observed lifetime to the fluorescence. Thus,

TABLE I. Low-lying electronic states of PO<sub>2</sub>.

State	$T_0/\text{cm}^{-1}$	$r_{\text{PO}}/\text{\AA}$	$\theta^\circ$	$\nu_1/\text{cm}^{-1}$	$\nu_2/\text{cm}^{-1}$	$\nu_3/\text{cm}^{-1}$	Reference
$2^2B_2$	30 378 <sup>a</sup>		Bent	933	396		Reference 20
$1^2B_1/{}^2\Pi_u$	28 685	1.5659	180	926	400	1319	Reference 28
$1^2B_1/2^2A_1/{}^2\Pi_u$	32 262 <sup>b</sup>	1.478	180	1046	187.7	1420	Reference 29
$1^2B_1/{}^2\Pi_u$	30 150		180				Reference 23
$1^2A_2$	8241	1.5425	107.04	1105	409	1208	Reference 28
	11 534	1.517	105.8	1269	459		Reference 29
$1^2B_2$	5055	1.5413	96.6	1068	381	1097	Reference 28
	9114	1.496	95.8	1333	428		Reference 29
$\tilde{X}^2A_1$	0	1.466	135.3	1090 <sup>c</sup>	377 <sup>c</sup>	1278 <sup>c</sup>	Reference 21
		1.464	135.14	1117	387		Reference 23
		1.446	134.4	1052	389	1338	Reference 28
				1048	396	1260	Reference 18

<sup>a</sup>The value of 30 378 cm<sup>-1</sup>, actually  $T_0$ , not  $T_e$ , was assigned based upon upper state line numbering, which has since been called into question (Refs. 21 and 28). Currently, there is doubt regarding the assignment of the observed spectrum (Ref. 20) to the  $2^2B_2$  state.

<sup>b</sup>An *ab initio* work (Ref. 29) considered the state to arise from a conical intersection between the  $1^2B_1$  and the  $2^2A_1$  states.

<sup>c</sup>Kawaguchi *et al.* (Ref. 21) assigned an uncertainty of 20 cm<sup>-1</sup> for  $\nu_1$  and  $\nu_2$ , while  $\nu_3$ 's uncertainty was much greater.

Hamilton proposed that the shorter-lived state, which he and Verma and McCarthy analyzed, is probably the linear  ${}^2B_1$  state calculated by Lohr, and the longer-lived state, whose contribution increases with higher excitation, derives mostly from high vibrational levels of the ground electronic state.

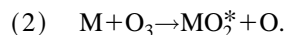
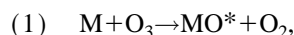
Stedman, however, observed broad CL in two different regions under different experimental conditions.<sup>25</sup> Stedman produced PO<sub>2</sub> by reacting phosphine (PH<sub>3</sub>) with O<sub>3</sub>/O<sub>2</sub>, O<sub>3</sub>/N<sub>2</sub>, O/O<sub>2</sub>, and other gas mixtures under multiple-collision conditions.<sup>25</sup> The spectra were very broad and mostly featureless. It is interesting to note that the gas mixtures involving O atoms did not yield any significant signal in the region from about 3000 to 4000 Å, while reactions with O<sub>3</sub> mixtures did give rise to a signal there. Since it is reasonable to expect that different precursors may lead to different electronic states, there may very well be two different states in this region.<sup>25</sup> In fact, the present investigation suggests that PO<sub>2</sub> can be formed in a nonlinear state that can readily emit radiation in this region, and the obvious candidate is a  ${}^2B_2$  state.

Andrews' and co-workers' matrix study of PH<sub>3</sub> reactions with O atoms to yield PO<sub>2</sub> has provided more information on the low-lying, emitting states. They attribute the matrix PO<sub>2</sub> spectra to a nonlinear  ${}^2B_2$  state. They do not rule out the possible existence of a linear  ${}^2B_1$  state as well,<sup>30</sup> but the  $B_1^2$  state of Hamilton was not populated in absorption. It is conceivable that the surrounding matrix of Ar may have hindered the PO<sub>2</sub> molecule from making the drastic geometry change from the bent ground state to a linear  ${}^2B_1$  upper state. Instead, the transition was to a bent  ${}^2B_2$  state.

The spectroscopy of the group VA monoxides, on the other hand, is more straightforward. Much more is known, and spectroscopic constants are available for most of the lower-lying electronic states of the monoxides.<sup>34</sup>

The primary motivation for this work, however, has not been to determine spectroscopic information, but rather to gain a better understanding of the chemiluminescent reactions involving P, Sb, and Bi atoms and dimers. This study

employed near single-collision conditions with the hope of limiting the number of possible mechanisms so that the salient mechanism(s) may be determined. To shed some light upon which mechanisms might be possible and which might not be, the thermochemistry of several potential steps have been calculated from existing data. The reactions have been generalized for the group VA elements: M=P, Sb, Bi. The following reactions would be first order with respect to O<sub>3</sub> pressure:



The following reactions would be second order with respect to O<sub>3</sub> pressure:

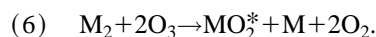
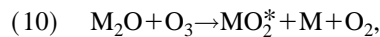
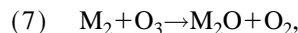
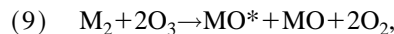
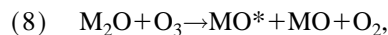
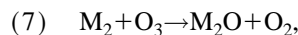
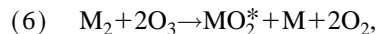
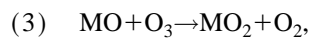
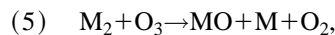
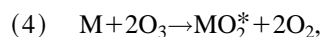
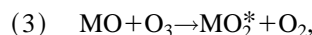
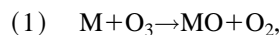


TABLE II. Standard reaction enthalpies<sup>a</sup> of atoms and dimers with O<sub>3</sub> (in eV).

Reaction	Reactant M:	P	Sb	Bi
First order in O <sub>3</sub>				
(1) M+O <sub>3</sub> →MO*+O <sub>2</sub>		-5.05±0.05	≧-3.34±0.05	-2.42±0.10
(2) M+O <sub>3</sub> →MO <sub>2</sub> *+O		-5.04±0.12	≧-1.90±0.50	-0.21±0.50
Two-step mechanism, second step				
(3) MO+O <sub>3</sub> →MO <sub>2</sub> *+O <sub>2</sub>		NA	≧-2.63±0.5	-1.86±1.0
(8) M <sub>2</sub> O+O <sub>3</sub> →MO*+MO+O <sub>2</sub>		NA	-2.2±1.0	-1.93±1.0
(10) M <sub>2</sub> O+O <sub>3</sub> →MO <sub>2</sub> *+M+O <sub>2</sub>		NA	-1.5±1.0	-1.37±1.1

<sup>a</sup>See the text for details on how these values were calculated.

Other reactions are possible, and were considered; however, they were excluded due to the fact that they are not exothermic enough to produce CL, or else require excessive bond rearrangement within a single step (such as M<sub>2</sub>+O<sub>3</sub>→MO+MO<sub>2</sub>). Also considered, but determined to be unimportant by experiments described here, was the two-step mechanism, which involved M<sub>2</sub>+O<sub>3</sub>→MO+M+O<sub>2</sub>, in which the M atom product subsequently reacts according to M+O<sub>3</sub>→MO+O<sub>2</sub>. The exothermicities were calculated upon well-accepted bond strengths (Huber and Herzberg<sup>34</sup> and JANAF<sup>35</sup>), where available. Also, Twarowski<sup>36</sup> and others<sup>37</sup> have determined bond strengths of several P-containing compounds, including PO<sub>2</sub>, although some still contained significant uncertainties. However, no data were available for SbO<sub>2</sub>, Sb<sub>2</sub>O, BiO<sub>2</sub>, and Bi<sub>2</sub>O. The unknown triatomic bond strengths were estimated from the ratio of the bond strengths in P-containing triatomic and diatomic molecules. The ratio was multiplied by the diatomic bond strength for Sb and Bi compounds. For example,  $D_0^\circ(\text{OM-O}) = D_0^\circ(\text{M-O})D_0^\circ(\text{OP-O})/D_0^\circ(\text{P-O})$ . Calculated standard enthalpies of reaction, at 0 K, are given in Table II. When the second step alone can produce electronically excited products, the enthalpy of the first step of a two-step mechanism is not critical, provided that the reaction is thermoneutral or exothermic.

An intriguing question to be addressed is why lighter elements in the group may lead readily to dioxide formation, while monoxides may be favored for heavier elements. One motivation for this investigation was to determine, given well-defined single-collision conditions, whether reactions to form monoxides are actually preferred over those forming dioxides, and also to determine the mechanisms that might be operable under multiple-collision conditions. Reactions with O<sub>3</sub> rather than O<sub>2</sub> were studied, since reactions with O<sub>2</sub> would not allow for significant dioxide formation within a single step because of the need for a stabilizing collision.

Also of interest are any differences in the reactivities of atoms and dimers of these group VA elements. Time-dependent CL experiments, in which the velocities of reacting group VA species are inferred, were considered as a means of determining the identity of reacting species (atoms or dimers), as well as evaluating any barriers to reaction. The appearance of any time-dependent CL signal at times other than those expected from an effusive beam, with a Boltzmann velocity distribution, may indicate either a barrier to reaction or possibly attractive forces that may increase reactivity. For instance, a barrier to reaction would select the

faster species within a beam, resulting in an observed peak shifted to earlier times when compared to the Boltzmann distribution.

## EXPERIMENT

Two different vacuum chambers were used for the dispersed chemiluminescence and for the time of flight (TOF) time-dependent experiments. These chambers were previously described,<sup>38,39</sup> but will be described, in part, here. Each vacuum chamber consisted of the separate subchambers, pumped by diffusion pump/mechanical pump pairs. The two subchambers were connected via a small slit allowing the effusive metal (or phosphorus) beam to enter the oxidizing subchamber. The diffusion pumps could achieve a background pressure of less than 10<sup>-6</sup> Torr within the chambers, providing single-collision conditions.

The CL from nascent products of exothermic reactions was monitored as both a function of time dependence<sup>38</sup> and of wavelength.<sup>39</sup> The time dependence was used to determine the identity of the reacting VA species (either atom or dimer) and potentially to determine the energy dependence of the reaction cross section. The dispersed CL was useful in determining the identity of the emitting product(s).

Some modifications to the beam source were made in order to achieve control over the composition of beams containing VA elements, some of which vaporize from the solid mostly as tetramers at the temperatures required to obtain vapor pressures from about 0.1 to 1.0 Torr. This pressure range is convenient for forming an effusive beam with the experimental apparatus. Since the tetramers do not appear to lead directly to observable products, measures were taken to increase the relative amounts of atoms or dimers by dissociating the tetramers.

So, a double oven, effusive beam source was used to control both total vapor pressure and the composition of the beam. By adjusting the temperature of the high temperature, or upper oven chamber, varying relative amounts of atoms and dimers could be selected. Tetramers could be virtually eliminated. The low-temperature chamber, or lower oven, was a molybdenum cylinder with a crucible for holding phosphorus or metal powder. This lower oven was radiatively heated with a W-mesh radiator, heated with a high-current ac power source that was previously described.<sup>40</sup> The upper oven was inserted into the lower oven through a hole in its side. The upper oven was a boron nitride tube, with a narrow (1 mm in diameter) cylindrical inner opening. The

upper oven was heated via a dc current run through a 1 mm diam tantalum wire. The wire was wrapped around the end of the upper oven several times.

Calibration with an optical pyrometer showed that the upper oven could be heated to temperatures in excess of 2000 K. While there was a small amount of heat leakage back to the lower oven, the lower oven could be reliably heated and temperature controlled by the radiator surrounding it. The lower oven was calibrated with a chromel–alumel thermocouple.

Bi dispersed-CL experiments were done without the use of a double oven since Bi has a tendency to form a greater proportion of atoms than other group VA elements at oven temperatures convenient for vaporization. Also, since the time-dependent experiments with Bi and O<sub>3</sub>, in which there was more control over atom/dimer proportions, showed that there are apparently no observable reactions involving dimers, it was unnecessary to conduct dispersed-CL experiments with a double oven source.

Ozone was generated from dry O<sub>2</sub> using a commercially available ozonator, from Ozoteq, Inc., model 25-0. A flow of about 3%–5% O<sub>3</sub> in O<sub>2</sub> was generated. However, a pure source of O<sub>3</sub> was desired for the low-pressure reactions that were to be the subject of this study. So, the O<sub>3</sub> was adsorbed selectively on freshly dried silica gel contained within a glass flask, cooled to dry ice temperatures with a dry ice/2-propanol slurry. Once a sufficient quantity of O<sub>3</sub> had been adsorbed, the silica gel/O<sub>3</sub> flask was connected to the vacuum chamber via a glass stem with a teflon needle valve to control O<sub>3</sub> vapor flow and pressure.

The time dependence of the signal was determined with the use of a chopping wheel that allowed pulses of the effusive beam down a fixed flight path, triggered the detection equipment, and determined the beam open zero time via detection of oven light. The chopping wheel and motor were previously described,<sup>38</sup> but the equipment used for detection had changed. The photomultiplier tube (PMT) in use was an EMI model 9816B with an S-20 photocathode response, and the output of the PMT was collected by a multichannel scalar (Turbo-MCS) from EG&G Ortec. The S-20 response of the PMT is insignificant beyond 8500 Å. The data were conveniently transferred to a personal computer for processing. Pulses of the metal (or P) effusive beam were created with chopping wheels rotated at 200–350 Hz, with either two or four narrow (2 mm wide) slots cut at the edge of the wheel, through which the beam passed. Beam pulses were 15–25 μs in duration. This finite temporal width was a source of some loss of resolution in the time-dependent spectrum, which was accounted for within computer simulations of the spectra. Another source of loss of time resolution within the spectrum was that the pathlength traveled by the reacting species could not be exactly defined. The detected image of the reaction/detection region under the PMT was not infinitely narrow. A 1 cm wide mask was placed over the cold cell, which better defined the region. Pathlengths of 16.6 and 18.3 cm were used. The width of observation, and thus the uncertainty, was 1 cm. This source of error in time was also accounted for within the simulation program.

Another problem with time resolution in the time-

dependent experiments of Sb and Bi occurred due to the large disparity in their masses when compared to that of O<sub>3</sub>. Ozone's room temperature speed distribution would be too broad compared to that of the metalloids and would become too large a contributor to the relative speed of the colliding pair. Thus, the resolution of the time-dependent spectra would be diminished to the point of being nearly useless for obtaining information about the collision energy dependence of reaction cross sections. Instead, measurements were made with a cold cylindrical scattering cell, 3.25 cm diam×3.66 cm high with a rectangular slit, 1.8 mm wide×7.7 mm high for beam entrance and a quartz window on top for CL viewing. This scattering cell was placed along the effusive beam axis and below the PMT. The cell was cooled to liquid nitrogen temperature by contact with an internal reservoir that was fed by a dewar external to the vacuum. The O<sub>3</sub> was passed through teflon tubing into the cell. In this way, the time-dependent resolution was dramatically increased for the slower beam species. This same cold cell was used with P+O<sub>3</sub> time-dependent experiments as well, since velocity resolution was improved in experiments with the cell. But its use was not as critical as with Sb and Bi experiments due to the lighter mass of P.

The vacuum chamber in which dispersed CL was observed was also previously described<sup>38,39</sup> but it too will be briefly described here. The chamber was mated to a  $\frac{3}{4}$  m monochromator equipped with a 300 line/mm diffraction grating. The exit slit of the monochromator was replaced with a liquid nitrogen cooled multichannel CCD detector, Princeton Instruments model LN/CCD-1152UV. The spectral response of the CCD/grating was strongest from 5500 to 7000 Å, but was significant from below 3000 Å to beyond 9000 Å. The resolution of this arrangement was limited to 1 Å, as each pixel corresponded to very nearly 1 Å, given the dispersion of the grating and monochromator pathlength. In these experiments, this limited resolution did not seem to obscure features because the spectra were generally broad and congested. The spectrum over 1150 Å was viewed simultaneously for each grating angle. Adjacent and overlapping spectral regions were joined by multiplying by an appropriate scaling factor so that the resulting two spectra had the same intensity in the overlap region. Random noise, spikes within the spectrum, which were caused by cosmic rays interacting with the CCD, was removed with a derivative filter program that was provided by the manufacturer.

In the dispersed-CL experiments, it became necessary to make a special inlet tube for the O<sub>3</sub> gas that was directed to the immediate area near the detection zone. The outlet of the tube was positioned about 1 cm from the intersection of the metal (or P) beam and the area beneath the collection optics to the monochromator. Concentrating the O<sub>3</sub> in this smaller region was thought necessary to avoid a large background light signal in the phosphorus reaction, which appeared to be from all parts of the chamber, not just in the area immediately surrounding the effusive beam (where one would expect a glow from CL reactions). Possibly this signal arose from O<sub>3</sub> reactions with phosphorus deposited on the walls of the chamber. The use of the O<sub>3</sub> inlet tube reduced this glow substantially.

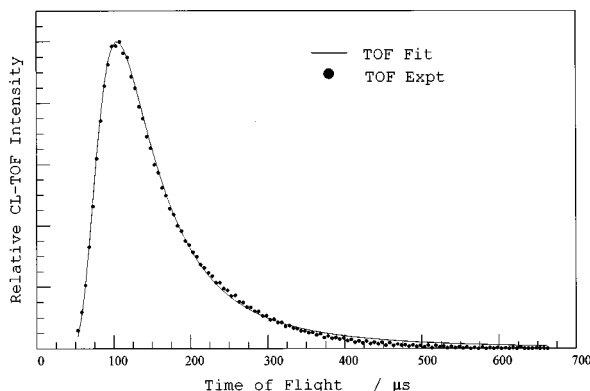


FIG. 1. The  $P+O_3$  CL intensity as a function of time. Dots are the experimental data, and the solid curve is the fit to  $\sigma_R \propto (E-V_0)^n/E$ .  $T(P)=1940$  K,  $P(O_3)=0.028$  mTorr, as measured in the chamber. The results of the fit were a negative barrier,  $V_0 = -10.4$  kJ mol $^{-1}$ , and the exponent  $n = 1.33$ .

The CL was observed under near-single-collision conditions, with  $O_3$  pressures on the order of 1 mTorr. It is not possible to give precise absolute pressures because of difficulties in achieving sufficient conductance between the cell and a gauge. Rather, relative pressures were determined by using a capacitance manometer from MKS Instruments, Inc., model 398HD, in conjunction with a digital display unit also from MKS, model 270B. The manometer measured the pressure in the chamber, but outside the cell. In the case of the time-dependent experiments, the cell pressure was calculated to be higher than the chamber pressure by a factor of about 75. In the case of dispersed-CL experiments, the ratio of the pressure in the reaction region to the chamber pressure was estimated to be considerably less than in the time-dependent experiments, but not precisely known.

## RESULTS

### $P+O_3$

The nascent products of the reaction between P and  $O_3$  were observed both through the dispersed CL and through the total CL intensity in the time-dependent experiments. Under different oven conditions, there may have been different proportions of atoms, dimers, and tetramers and time-dependent measurements offer a way to distinguish them.<sup>38</sup> Fortunately, the presence of tetramers was, for all practical purposes, eliminated. However, in the case of phosphorus, it was not possible to select exclusively atoms, even for upper oven temperatures near 2000 K. At that temperature, only a few percent of atoms were attainable.<sup>41</sup> Least squares fits of the observed time-dependent signal to expected forms, depending upon different models for the form of the reaction cross section, were able to confirm that the reactant that gave rise to the signal was the atom and not the dimer of P. The time-dependent signal was fit successfully for P atoms as a reactant, but not P dimers. This result is also consistent with the fact that the signal was observed to decrease as the upper oven temperature was lowered, giving fewer atoms, but more dimers. The time-dependent signal, along with the results of the best fit are shown in Fig. 1. The cross-section form used

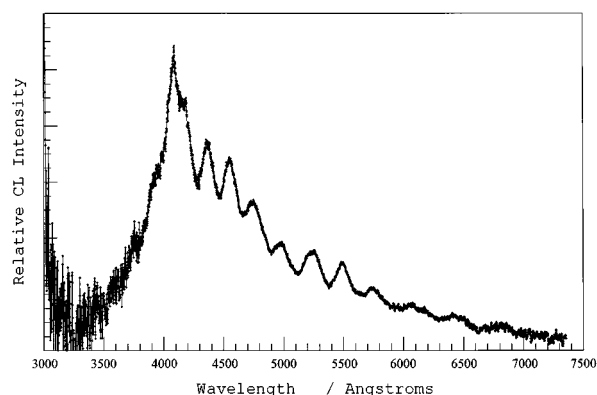


FIG. 2. The  $P+O_3$  net CL corrected for spectral response. The spectrum was taken with a resolution of 10 Å.  $T(P)=2060$  K,  $T(O_3)=293$  K, and  $P(O_3) \approx 0.05-0.09$  mTorr. The CL signal is believed to be due to atom reaction, although the beam was only about 1%–2% atoms, with the remainder being dimers (Ref. 41).

in the fit was a microcanonical transition state theory model as described by Gonzales Ureña.<sup>42,43</sup>  $\sigma_r \propto (E-V_0)^n/E$ , where  $V_0$  is the barrier to reaction and  $E$  is the collision energy. The resulting values were  $V_0 = -10.4$  kJ/mol and  $n = 1.33$ . Other cross sections form, including a hard spheres–line of centers model, did not yield fits of similar quality. The time-dependent signal was also studied as a function of  $O_3$  pressure. The data, for chamber pressures of 0.04 mTorr and lower, were successfully fit to a first order in  $O_3$  pressure dependence. Higher pressures exhibited attenuation.

Figure 2 shows the dispersed CL for the  $P+O_3$  reaction. The  $P_n$  source's upper oven temperature was roughly 2060 K, based upon pyrometric calibrations, giving a relative amount of P atoms of about 1%–2%,<sup>41</sup> the rest being the apparently unreactive dimers. The background was subtracted out of the spectrum, and then the net signal was corrected for a spectral response of the monochromator/grating/CCD detection system. The spectral response was determined from measured intensities from previously calibrated standard lamps. This experiment was conducted with a resolution of 10 Å. The spectrum covers the range of about 3000 to beyond 7000 Å. This range roughly coincides with Stedman's spectra,<sup>25</sup> although the spectrum from this study does not have nearly as much intensity at long wavelengths as Stedman's. PO cannot account for the regular pattern in the spectrum. The observed smooth oscillations are believed to be due to  $PO_2$ .

### $Sb_n+O_3$

The  $Sb_n+O_3$  results were decidedly different from those of  $P+O_3$ . The biggest difference arose in time-dependent experiments (see Fig. 3). The time-dependent spectra show two peaks whose intensities relative to each other depend markedly upon  $O_3$  pressure. It is apparent that there was more than one reaction channel, at least one channel for each peak. The  $Sb_n+O_3$  early and late time-dependent peaks were fit to first- and second-order dependences in the observed  $O_3$  chamber pressures, respectively. At lower pressures, the intensities were found to fit the orders in  $O_3$  with good agree-

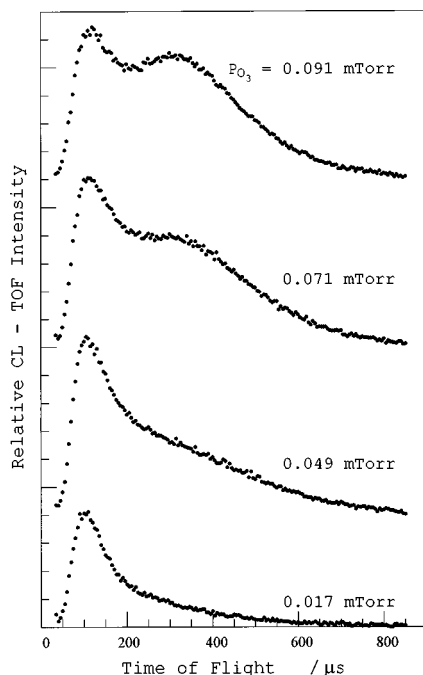


FIG. 3. The  $\text{Sb}_n + \text{O}_3$ ,  $n=1, 2$  (99% atoms<sup>41</sup>) CL intensity as a function of time for a series of  $\text{O}_3$  chamber pressures. Note the growth of the second peak relative to the earlier peak with higher  $\text{O}_3$  pressures.  $T(\text{Sb}_n) = 1960$  K and  $T(\text{O}_3) = 78$  K.

ment. At pressures greater than about 0.02 mTorr (in the chamber), some attenuation in the intensity was observed. The first- and second-order (in  $\text{O}_3$ ) peaks fit very well to the functional form:  $I \propto P^n e^{-\alpha P}$ ; where  $I$  is the observed intensity,  $P$  is the measured pressure of  $\text{O}_3$ ,  $n$  is the order with respect to  $\text{O}_3$ , 1 for the earlier peak, and 2 for the later peak, and  $\alpha$  is an attenuation coefficient. As will be discussed below in more detail, a mechanism involving  $\text{Sb}_2$  is more likely to be associated with the second-order (in  $\text{O}_3$ ) process, while the first order in  $\text{O}_3$  process, corresponding to the earlier peak, is more likely to involve Sb atoms. Both Sb atoms and dimers were present under the conditions in which the time-dependent spectra in Fig. 3 were taken. The  $\text{Sb}_n$  source upper oven was at about 1960 K, giving about 99% atoms, the rest dimers.<sup>41</sup> One would expect atoms to lead to earlier peaks than dimers, since their most probable velocity is larger by a factor of  $\sqrt{2}$ . When the upper-oven temperature was lower, yielding a higher ratio of dimers to atoms, the earlier peak vanished relative to the later peak.

Comparisons of the later peak to expected atom and dimer Boltzmann distributions shown in Fig. 4 are consistent with dimer reactants; however, by itself, such a comparison is not conclusive. The ambiguity arises from the possibility that the early peak, and potentially the later peak, might correspond to only fast atom or fast dimer reactants. The faster species might be selected over the slower species by a very large energy barrier to reaction. Lowering the upper oven temperature could drastically reduce the number of fast, reacting species (either atom or dimer), thus accounting for the loss in time-dependent intensity. For this reason, time-dependent experiments were conducted at a given total vapor pressure of all  $\text{Sb}_n$  species. The upper-oven temperature was

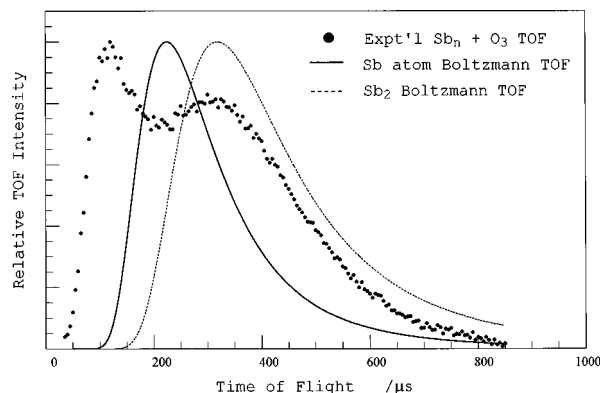


FIG. 4. The  $\text{Sb}_n + \text{O}_3$ ,  $n=1, 2$  (99% atoms<sup>41</sup>) CL intensity as a function of time for  $P(\text{O}_3) = 0.091$  mTorr,  $T(\text{Sb}_n) = 1960$  K, and  $T(\text{O}_3) = 78$  K. Experimental data (the dots) are compared to the atom Boltzmann velocity/time distribution (a solid curve) and to the dimer Boltzmann distribution (a dashed curve).

varied to give different amounts of atoms and dimers. The ratio of early to late peaks was compared for these spectra with the different atom to dimer proportions. As the dimer pressure was increased, the intensity of the later peak increased as well.

As with  $\text{P} + \text{O}_3$ ,  $\text{Sb}_n + \text{O}_3$  time-dependent spectra were simulated and compared to predicted models of reaction cross sections for an effusive beam velocity distribution. The fits to the early peak were unsuccessful; however, the later peak was successfully fit to a hard spheres–line of centers model, with  $\text{Sb}_2$  as the initial reactant, and allowing for a time delay for the occurrence of a second collision. For an  $\text{O}_3$  temperature of 78 K, the line of centers barrier to reaction was  $-1.85$  kJ mol<sup>-1</sup>, and the time delay was  $5.1$   $\mu\text{s}$ . (See Fig. 5.)

So it appears that  $\text{Sb}_2$  contributed to the later time-dependent peak. But we cannot rule out some atom contribution to the later peak. Nor can we rule out dimer contribution to the earlier peak. But it appears that the earlier peak is primarily due to the Sb atom reaction.

Figure 6 shows the dispersed-CL spectrum from  $\text{Sb}_n$

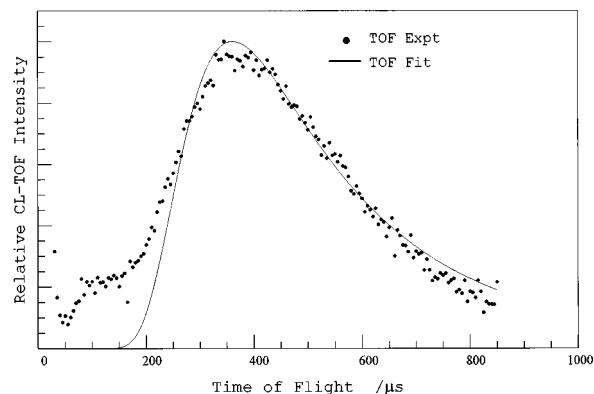


FIG. 5. The  $\text{Sb}_2 + \text{O}_3$  time-dependent experimental data (dots) fit to a hard spheres/line of centers cross section,  $\sigma_R \propto (E - V_0)/E$  (solid curve), with a time delay to allow for a secondary collision with  $\text{O}_3$ . The results of the fit were a negative barrier,  $V_0 = -1.85$  kJ mol<sup>-1</sup>, and the time delay =  $5.1$   $\mu\text{s}$ .  $T(\text{Sb}_2) = 1675$  K,  $T(\text{O}_3) = 78$  K, and  $P(\text{O}_3) = 0.039$  mTorr. The beam was composed of 11%  $\text{Sb}_2$  and 89% atoms (Ref. 41).

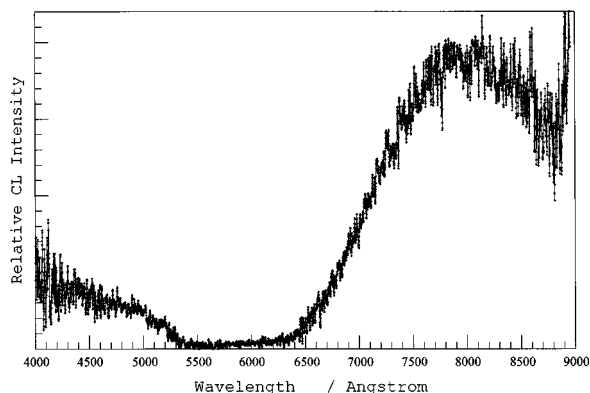


FIG. 6. The  $\text{Sb}_n + \text{O}_3$ ,  $n=1, 2$  (85% atoms<sup>41</sup>) not CL intensity corrected for the spectral response.  $T(\text{Sb}_n)=1800$  K,  $T(\text{O}_3)=293$  K,  $P(\text{O}_3)=0.04\text{--}0.06$  mTorr. The long-wavelength CL signal is probably due to  $\text{SbO}_2$ . The spectrum was taken with a resolution of  $30 \text{ \AA}$ .

+  $\text{O}_3$ . This spectrum was taken at  $10 \text{ \AA}$  resolution. The  $\text{Sb}_n$  source upper oven temperature was  $1800$  K, yielding roughly 85% atoms.<sup>41</sup> At the time of the experiments the pressure was thought to be sufficiently low to make two-step mechanisms unlikely; however, due to an inability to measure the absolute  $\text{O}_3$  pressure in the TOF cell, and also in the detection region of the dispersed-CL vacuum chamber, we cannot be certain that only a first order in  $\text{O}_3$  process was responsible for the observed CL. The  $\text{O}_3$  chamber pressure for this spectrum was on the order of  $5 \times 10^{-5}$  Torr; however, the  $\text{O}_3$  pressure at the antimony beam was greater and may have been sufficient to allow for secondary collisions with  $\text{O}_3$ . Also, since the dispersed-CL detection system was more sensitive to longer-wavelength fluorescence than the PMT used in the time-dependent measurements, mechanisms second order in  $\text{O}_3$  yielding long-wavelength fluorescence could contribute to the dispersed-CL signal at lower pressures.

Franck-Condon Factors (FCFs) were calculated as earlier<sup>44</sup> for  $\text{SbO}$ 's two lowest transitions,  $A_2^2\Pi_{1/2} \rightarrow X_1^2\Pi_{1/2}$  and  $A_1^2\Pi_{3/2} \rightarrow X_2^2\Pi_{3/2}$ ,<sup>34</sup> to see if  $\text{SbO}$  is responsible for the CL. According to the FCFs, there should be some intensity around  $6000 \text{ \AA}$ , while longer wavelengths should not have much greater intensity. It appears that there is some  $\text{SbO}_2$  contributing to this spectrum because of the way the signal increases at longer wavelengths. If the FCFs for  $\text{SbO}$  are multiplied by a broad thermal distribution of the known upper vibronic states that are energetically allowed (in the  $A_2$  and  $A_1$  states), then there still is no indication that  $\text{SbO}^*$  could be responsible for all of the emission in the region  $7000\text{--}9000 \text{ \AA}$ . Even if it were so, there would still be  $\text{SbO}^*$  emission around  $6000 \text{ \AA}$ , where there is none.

### Bi+O<sub>3</sub>

As for phosphorus and antimony, bismuth reactions were studied as functions of time dependence and  $\text{O}_3$  chamber pressure. Spectra shown in Fig. 7 are very similar to those for the  $\text{Sb}_n$  reactions. Both series of spectra include two peaks, with the later peak obviously exhibiting a higher dependence upon  $\text{O}_3$  pressure than the earlier peak. However, other important details were discovered that contrast the  $\text{Sb}_n$

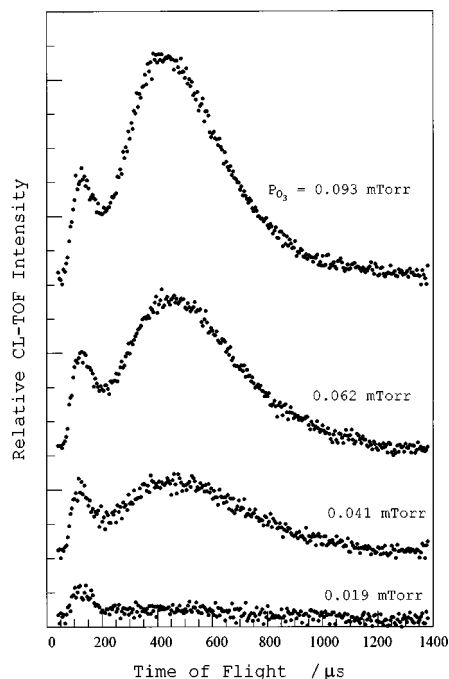


FIG. 7. The  $\text{Bi} + \text{O}_3$  (99.8% atoms<sup>41</sup>) CL intensity as a function of time for a series of  $\text{O}_3$  chamber pressures. Note the growth of the second peak relative to the earlier peak with higher  $\text{O}_3$  pressures.  $T(\text{Bi})=1800$  K and  $T(\text{O}_3)=78$  K.

spectra. Dimers are extremely unlikely to be the reactant for either peak since the spectra shown were taken with an upper oven temperature of  $\sim 1800$  K, which gave virtually all atoms in the beam. Figure 8 shows the experimental time-dependent data of  $\text{Bi}_n + \text{O}_3$  reaction (dots connected by a solid curve), with the later peak fit by a computer simulation to the cross-section form (dashed curve):  $\sigma_R \propto E^n$ , where  $E$  is the collision energy, and  $n$  is a fitting parameter. The fit also allowed for a time delay to account for a secondary collision, as previously described for  $\text{Sb}_2 + \text{O}_3$  time-dependent simulations. The result of the fit yielded  $n = -1.45$  with a time delay to the secondary reaction of  $1.17 \mu\text{s}$ . For comparison,

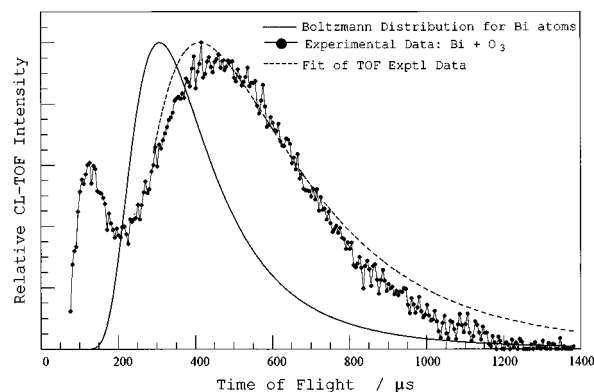


FIG. 8. The  $\text{Bi} + \text{O}_3$  time-dependent experimental data (dots) fit to a cross section form:  $\sigma_R \propto E^n$  (a dashed curve), with a time delay of  $1.17 \mu\text{s}$ , allowing for a secondary collision. The experimental data and the fit are compared to the atom Boltzmann velocity/time distribution (a solid curve).  $P(\text{O}_3)=0.062$  mTorr, as measured within the chamber,  $T(\text{Bi})=1800$  K, and  $T(\text{O}_3)=78$  K. The beam was 99.8% atoms (Ref. 41).

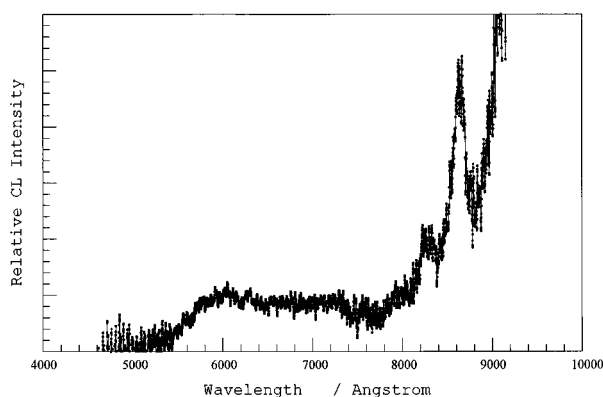


FIG. 9. The Bi+O<sub>3</sub>, net CL corrected for spectral response.  $T(\text{Bi})=1180$  K,  $T(\text{O}_3)=293$  K,  $P(\text{O}_g)=0.1\text{--}0.2$  mTorr. The long-wavelength CL signal is not due to BiO. Beam composition was approximately 40% atoms, 60% dimers<sup>41</sup>; however, time-dependent experiments have shown dimers to be unreactive. The spectrum was taken with a resolution of 30 Å.

the arrival time of Bi atoms (solid curve) governed by a Boltzmann velocity distribution is also displayed.

Bismuth + O<sub>3</sub> CL intensity was also studied as a function of wavelength at 1180 K in a single chamber oven. There were approximately 40% atoms, 60% dimers present.<sup>41</sup> The dispersed CL spectrum, displayed in Fig. 9, is mostly featureless, with the exception of two peaks around 8500 Å. The intensity, compared to that of the P<sub>n</sub> reaction, was quite low. The CL intensity data were corrected for spectral response after the background was removed. Only at very long wavelengths (beyond 8500 Å) did the intensity grow; however, spectral response was falling very rapidly at these wavelengths. Extraneous large counts from stray light or noise, magnified by division by a very low spectral response value at long wavelengths, might account for some long-wavelength intensity, but not for the distinctive peaks. As was the case with antimony, the O<sub>3</sub> pressure may have been high enough at the bismuth beam to allow for secondary collisions of the monoxide product with O<sub>3</sub>.

## DISCUSSION

Verma and McCarthy<sup>20</sup> reported that they observed absorption in PO<sub>2</sub> from the ground  $^2A_1$  state to a  $^2B_2$  state. Their assignment of their spectrum to the,  $2^2B_2$  state was based upon an apparent predissociation and similarities in structure to NO<sub>2</sub>. Hamilton<sup>23</sup> found that there was no predissociation by examining lifetimes of different vibrational levels. He proposed that Verma and McCarthy's spectrum as well as his LIF spectrum arose from a linear  $^2B_1(^2\Pi_u)$  state. Hamilton's assignment was influenced by the theoretical prediction of Lohr<sup>27</sup> that a linear state exists with an origin near 30 000 cm<sup>-1</sup> above the ground state. Another point presented by Hamilton for consideration was that a vertical transition from the linear upper state to a linear geometry of the ground state, would have a maximum at around 450 nm, which is in agreement with his observations. Still, Hamilton was unable to state definitively that the excited state was the linear  $^2B_1$  state.<sup>23</sup> He believed that part of his spectrum was mixed with high-lying vibrational levels of the ground state, resulting in long lifetimes and low intensities. Other parts of his spec-

trum may have resulted from mixing the  $^2B_1$  with states other than the ground electronic state. In a more recent *ab initio* treatment, Buenker and co-workers<sup>28</sup> have also found the linear  $1^2B_1$  state in the region, but showed that just slightly higher the  $2^2B_2$ ,  $2^2B_1$ , and  $2^2A_1$  states are expected to have origins, all with strongly allowed transitions to the ground electronic state.

On the other hand, according to the Franck-Condon principle, one would expect LIF excitation to occur to a state with a geometry closer to that of the ground state, if there were more than one state at the excitation energy. In other words, the absorption cross section from the bent ground state to a linear excited state would be quite small.<sup>30</sup> The matrix studies by Andrews and co-workers<sup>30-33</sup> suggest the presence of a bent  $^2B_2$  state in that very same region, and support Verma and McCarthy's<sup>20</sup> assignment of the spectra in the region around 3000 Å. Transitions involving large geometry changes, such as linear to bent transitions, are unlikely within a matrix, where there is little space for geometry changes, especially with another nearby state having a geometry similar to that of the ground state. If the  $2^2B_2$  state is not assigned to the upper state in either Verma and McCarthy's or Hamilton's experiments, then one is faced with a puzzle as to why a transition, the  $1^2B_1 \rightarrow \tilde{X}^2A_1$ , with much smaller oscillator strength according to theoretical results,<sup>28</sup> would be observable instead.

Presuming that Hamilton's assessment that the  $1^2B_1$  state, being heavily perturbed, was predominantly the state to which he was exciting, there may still be another state in the same region that might have given rise to emission under other conditions. The question is whether a second state was produced in the P+O<sub>3</sub> reaction, or whether the present study has observed the  $1^2B_1$  state.

Stedman and co-workers<sup>25</sup> observed CL from about 2800 to 8000 Å from reactions involving PH<sub>3</sub> and O<sub>3</sub>. They associated two different spectral regions with different emitting states (or different product molecules). The intensity of the short- and long-wavelength regions depended differently on the amount of O<sub>3</sub> present, as well as the identity of the carrier gas (O<sub>2</sub> or N<sub>2</sub>).<sup>25</sup>

Our dispersed-CL spectrum of the P+O<sub>3</sub> reaction showed a regular spacing of peaks that are not attributable to PO. The lowest-energy transition in PO, the  $B^2\Sigma^+ \rightarrow X^2\Pi_r$ , has a  $T_0=30\,695$  cm<sup>-1</sup>,<sup>34</sup> which corresponds to a wavelength of 3258 Å, but the spectrum in Fig. 2 has no discernable structure, as would be typical of diatomic vibronic transitions, until wavelengths longer than 4080 Å. Transitions from the A state, with  $T_e=40\,407$  cm<sup>-1</sup>,<sup>34</sup> would occur at even shorter wavelengths. Nor can the peaks from the P+O<sub>3</sub> CL be assigned to stretching mode progressions in transitions from previously analyzed excited states of PO<sub>2</sub> to the ground state.

If a large number of vibrational levels within the upper electronic state could be populated, then one would not expect such a regular emission pattern as observed. The presence of predissociation of many of the energetically possible states, by reducing the number of bound vibrational levels, could have the effect of simplifying the spectrum. The energetics shown in Table II for reaction (1) imply that sufficient

energy is available to dissociate  $O_2$  ( $D_0^\circ = 5.116$  eV) if the average energy of reactants of 0.22 eV is made available. Hence, our experimental conditions can form  $PO_2$  very close to the  $PO+O$  dissociation limit if translational energy is small. So it is reasonable to expect that only a very limited number of states of  $PO_2$  might survive, and most of those could be quasibound by rotational or potential barriers to dissociation. Similar oscillatory structure has been seen in bound to free transitions<sup>45</sup> and transitions from weakly bound excited states.<sup>46</sup>

If a small number of vibrational states are populated in the electronically excited  $PO_2$  found in our experiments, then the oscillatory structure in the CL spectrum may be caused by periodicity in the magnitude of FCFs in transitions to a progression of the ground state bending or stretching modes. The oscillation spacing of  $\approx 1000$   $cm^{-1}$  corresponds to slightly less than three bending or slightly less than one symmetric stretching quanta. Because the lower levels in the transitions at these wavelengths would have to be well above the ground electronic state origin, we cannot assign any particular levels. On the basis of geometry differences between the calculated excited state and the ground state, one would expect progressions in bending to be longer than stretching.

Another possible explanation for the  $PO_2$  dispersed-CL spectrum is that the observed emission might occur to two distinct lower states, the  $\tilde{X}^2A_1$  and the  $1^2B_2$  states. The short-wavelength part of the spectrum, corresponding to the greater emission energies, would correspond to transitions to the ground state. The longer-wavelength section of the spectrum would correspond to emission down to the  $1^2B_2$  state. Emission from a narrow vibrational population distribution within the upper state would likely give a simple and uncongested spectrum. If one interprets the high-frequency onset of oscillations in our spectrum around 26 000  $cm^{-1}$  as a transition between the lowest level of an unknown upper state and the  $1^2B_2$  state, and adopts the calculated  $1^2B_2T_e$  of 9114  $cm^{-1}$  (Table I), then the upper state  $T_e$  would be about 35 000  $cm^{-1}$  (4.34 eV). We note that Buenker and co-workers<sup>28</sup> have predicted vertical transitions from the ground state to  $2^2B_1$  and  $2^2A_1$  states at 4.56 and 4.64 eV, respectively.

What is striking about our results is the absence of  $PO$  fluorescence. One possible explanation as to why reaction (2) should be the only CL channel is that reaction (1) may be occurring but most of the excess energy ends up not in  $PO$ , but in dissociated  $O_2$ . Just such a process has been shown to occur in the reaction  $Bi_2+F_2 \rightarrow BiF+Bi+F$ .<sup>47</sup> Processes like this may be driven by the high density of states that are opened by accessing three unbound fragments.

Antimony +  $O_3$  time-dependent spectra have shown peaks apparently corresponding to both atom and dimer reactions. Strikingly, these two separate peaks were observed together, within the same scan, under certain experimental conditions: temperatures that provided significant proportions of both  $Sb$  dimers and atoms, and  $O_3$  pressures that were sufficiently great for secondary collisions to occur. Time-dependent experiments may possess only one maximum in intensity, even if two reaction channels contribute to the total intensity. The time-dependent profile from each re-

action channel may significantly overlap the other.

It has been observed by varying the  $O_3$  pressure that the later peak is of higher order with respect to  $O_3$  than the reaction(s) accounting for the earlier peak. See Fig. 3. In fact, the early peak, believed to be primarily due to fast atoms, has been fit to first-order dependence in  $O_3$ . The later peak, believed to be mostly due to dimers, has been fit to second-order dependence in  $O_3$  and is clearly not first order. At low pressures, the early peak survives, while the later, higher-order peak vanishes. Thus, the early peak appears to be predominantly due to reaction (1) or (2). The later peak appears to be mostly due to one or more of the two-step mechanisms involving  $Sb_2$  as a reactant within the first step. Specifically, the mechanism would involve reactions (5)+(3), (7)+(8), or (7)+(10).

Under other oven conditions, where virtually exclusive amounts of either atoms or dimers of  $Sb$  may be produced, the peaks have been isolated and shown to be mostly due to atoms in one case, and dimers in the other. Simulation of the time-dependent spectra in the case of antimony reactions has been completed with limited success. Attempts to fit the presumed  $Sb$  atom +  $O_3$  signal were unsuccessful. The simulated early peak arrived significantly later than the observed early peak. It is believed that very fast atoms are contributing to reaction leading to the early peak. From Fig. 4, one can see that there are very few atoms present (<1% of the maximum in the distribution) that have sufficient velocity to reach the detection zone at the time of the early peak.

Simulations are impossible at these high velocities because of uncertainties in the actual velocity distribution and the finite time and space resolution of the detection system. Simple estimates using the square of the ratio of observed arrival times for the early peak and the energy of the atoms calculated to arrive according to the Boltzmann distribution in Fig. 4, give a barrier to reaction of roughly 50  $kJ mol^{-1}$ .

In the case of  $Sb+O_3$ , the dispersed CL indicates the probable formation of two distinct products,  $SbO^*$  and  $SbO_2^*$ . The long-wavelength CL signal, commencing at 6500 Å, is thought to be  $SbO_2^*$ , while the short-wavelength CL, from below 4000 to 5300 Å, is thought to be  $SbO^*$ . (See Fig. 6.) The short-wavelength emission appears in the same region as the  $SbO$   $B^2\Sigma^+ \rightarrow X_1^2\Pi_{1/2}$  and  $B^2\Sigma^+ \rightarrow X_2^2\Pi_{3/2}$  with origins around 3776 and 4130 Å.<sup>34,48</sup> respectively. Vibronic transitions of higher quanta within given sequences would extend to longer wavelengths since the ground state vibrational frequencies are significantly larger than the  $B$  state frequencies.<sup>34</sup> The  $A \rightarrow X$  transitions also have some Franck-Condon intensity within the short-wavelength region. The  $A \rightarrow X$  transitions might account for some of the CL intensity here; however, as mentioned above, there is no CL intensity at other wavelengths where there is some Franck-Condon intensity for the  $A \rightarrow X$  transitions.

Similarly to  $Sb$ , the  $Bi+O_3$  reaction also exhibits this same two peak time-dependent signal. And similarly to  $Sb$ , the intensity of the later peak is observed to be of higher order in  $O_3$  than the earlier peak. But in contrast to the  $Sb+O_3$  CL/time-dependent spectra, the later peak is not principally due to dimers, but rather to atoms. At higher temperatures, where dimers are absent, both peaks still appear. The

higher-order O<sub>3</sub> pressure dependence indicates a two-step mechanism, most likely the one involving reactions (1) and (3), with BiO as an intermediate.

The electronically excited product formed in reaction (1) may require the faster part of the Bi atom velocity distribution because there is a barrier to forming the observed states. In fact, the earlier peak of the time-dependent spectrum was not successfully fit. Examination of Fig. 8, with the Bi atom Boltzmann arrival times, shows that the early time-dependent peak just simply arrives much earlier than most Bi atoms. The Bi atom distribution is not well enough known at the flight times for the earlier peak to be fit. Clearly, fast atoms with enough energy to surmount a barrier of approximately 40 kJ mol<sup>-1</sup>, did give rise to CL when the vast majority of the atoms did not lead to first order in O<sub>3</sub> CL. The value of 40 kJ mol<sup>-1</sup> for the barrier was arrived at in the same way as with Sb.

The dispersed-CL spectrum taken at low O<sub>3</sub> pressure is believed to be predominantly due to the first order in O<sub>3</sub> process, producing BiO. Inspection of the Franck-Condon Factors (FCF) for the BiO A→X<sub>1</sub> transition suggests that the BiO spectrum should be very broad. The FCFs are relatively strong for emission wavelengths, commencing at ~5000 Å and continuing to longer wavelengths, including beyond 9000 Å. The peaks at 8650 and 8250 Å, however, do not correspond to any particularly strong FCFs in BiO, and may be indicative of emission by electronically excited BiO<sub>2</sub>, which is thought to be the product of the second order (in O<sub>3</sub>) reaction. We are not aware of any previous observations of electronic spectra of this molecule.

Although the observed peak at 8650 Å does coincide with the O<sub>2</sub> b <sup>1</sup>Σ<sub>g</sub><sup>+</sup>→X <sup>3</sup>Σ<sub>g</sub><sup>-</sup> (0-1) transition, the (0-0), (1-0), and (1-1) peaks in the b→X electronic transition are not present. And an extremely long lifetime for the b→X transition would rule out detectability of O<sub>2</sub> b <sup>1</sup>Σ<sub>g</sub><sup>+</sup> in our apparatus.

The dispersed-CL and time-dependent spectra presented for O<sub>3</sub> reactions with Sb and Bi atoms, but not P atoms, show evidence for monoxide formation. All three elements show evidence for dioxide formation, although O<sub>3</sub> pressure dependences for each of the reactions indicate different mechanisms leading to the dioxides. P+O<sub>3</sub> seem to form PO<sub>2</sub><sup>\*</sup> within a single, possibly concerted, step. This process is much more favorable than any other to form PO<sup>\*</sup>. The long-wavelength CL (6500–9000 Å) indicates the formation of SbO<sub>2</sub><sup>\*</sup>. Uncertain O<sub>3</sub> pressures compel us to consider one- and two-step mechanisms. So, it appears that Sb<sub>2</sub>+O<sub>3</sub> form SbO<sub>2</sub><sup>\*</sup> through a two-step mechanism: (5)+(3) or (7)+(10), and possibly Sb+O<sub>3</sub> reacts via (2). There is also a possible atom mechanism reacting through (1)+(3). Bi+O<sub>3</sub> also appears to form BiO<sub>2</sub><sup>\*</sup> through the two-step mechanism comprised of reactions (1)+(3).

Questions arise regarding P atom reactivity relative to that of Sb and Bi. Why does P not appear to react with O<sub>3</sub> to form PO, while Sb and Bi do react to form their excited monoxides? And why do Sb and Bi atoms not appear to form their dioxides within a single step as strongly as P does? A partial answer to the first question is that P atoms are very reactive given all the open valences on the atom, and if it is

close enough to the second end O atom to experience any interactions, the P is very likely to bond to an additional O atom. Perhaps the only reaction channel that might lead to PO<sup>\*</sup> formation would require an extremely narrow end-on approach of the P toward an end O atom of O<sub>3</sub>. PO<sub>2</sub><sup>\*</sup> formation, on the other hand, may occur for orientations in which the P approaches only slightly off the direct-line approach to the end atom. It is also conceivable that the P–O<sub>3</sub> complex may rearrange fast enough for P to interact with a second O atom from the O<sub>3</sub> molecule. Also, as noted earlier, it may simply be that PO<sup>\*</sup>+O<sub>2</sub> formation just cannot compete with PO+2O and PO<sub>2</sub><sup>\*</sup>+O formation. Since the observations of this paper apply only to electronically excited products, future experiments using LIF detection of ground electronic state products will be necessary to see if the results generalize to all monoxide and dioxide products.

Phosphorus' reactivity may explain why PO<sub>2</sub><sup>\*</sup> is observed, while PO<sup>\*</sup> is not, but it does not explain the lack of any strong preference for Sb and Bi atoms to form their dioxides exclusively over their monoxides. In the case of Bi atoms, reaction (2) can simply be ruled out on the basis of its exothermicity (or lack thereof) found in Table I, -0.21±0.5 eV. Clearly, for Bi, reaction (2) would not release enough energy to yield any CL. The reactivity of Sb is not so conveniently explained, especially since energetically possible, two-step mechanisms, possibly involving Sb<sub>2</sub> and potentially leading to long-wavelength CL (Fig. 6) from SbO<sub>2</sub><sup>\*</sup>, can neither be ruled in nor ruled out.

If the long-wavelength CL signal in the antimony reaction is due to a two-step mechanism, then an explanation for the lack of single-step SbO<sub>2</sub><sup>\*</sup> formation through reaction (2) is needed. Consideration of the geometries of dioxides of P, Sb, and Bi compared with that of O<sub>3</sub> within its ground state and of potential transition states offers some insight. Unfortunately, we have not been able to locate geometries for SbO<sub>2</sub><sup>\*</sup> and BiO<sub>2</sub><sup>\*</sup>, but Table I gives them for PO<sub>2</sub>. The geometries for PO<sub>2</sub> and O<sub>3</sub> are depicted in Fig. 10. It shows that geometries of PO<sub>2</sub> can easily overlap the geometry of O<sub>3</sub> with a central approach of the P atom toward O<sub>3</sub>. Among possible electronic environments of the P–O<sub>3</sub>/PO<sub>2</sub>–O system, those with least molecular rearrangement would be more likely to form, corresponding to lower-energy crossings. Since the identity of the excited state of PO<sub>2</sub><sup>\*</sup> responsible for emission is uncertain, we compare the known geometries of some of the lower states of PO<sub>2</sub>. The P–O bond lengths within PO<sub>2</sub> would need to be displaced by only about 0.28 Å for the  $\tilde{X}^2A_1$  ground state or by less than 0.07 Å for the <sup>1</sup>2B<sub>2</sub> state of PO<sub>2</sub> to correspond to the equilibrium geometry of ground state O<sub>3</sub>. If one were to consider the bond lengths as fixed, then the bond angle within PO<sub>2</sub> would be displaced from its equilibrium value by 27° for the ground state, or by 5.6° for the <sup>1</sup>2B<sub>2</sub> state. The linear <sup>1</sup>2B<sub>1</sub> state of PO<sub>2</sub> would require drastic geometry changes by either 0.47 Å or 91°. These comparisons suggest that abstraction of the two end oxygen atoms by the P atom might proceed more readily than through other mechanisms with transition states of other geometries. Furthermore, suggestive of a small barrier is the fact that the O<sub>3</sub> molecule can be characterized as a "diradical" with an unpaired electron on each end atom.<sup>49</sup>

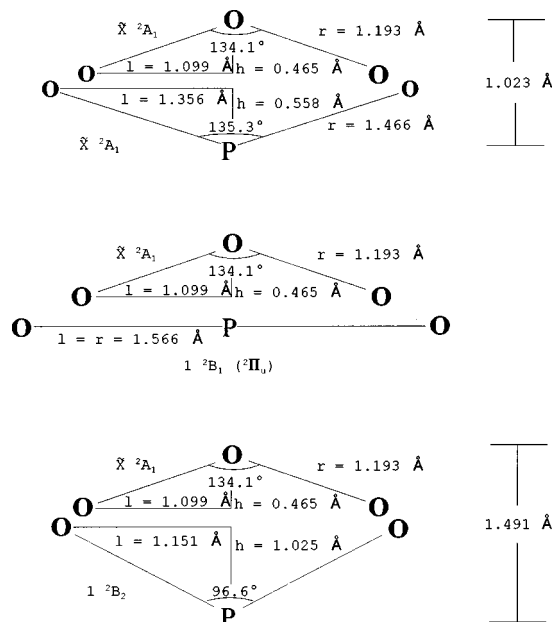


FIG. 10. Geometries of ground state  $O_3$  reactant compared to product  $PO_2$  in some of the energetically accessible electronic states. The transition state involving the four atoms would likely be somewhere between the  $O_3$  and one of the  $PO_2$  geometries. Of the three states of  $PO_2$  depicted, the  $1^2B_2$  appears to be the one most likely to form, on the basis of geometry, and most similar to an expected transition state for a side approach of the P atom. Note that the diagrams are not necessarily to scale, although they are generally reflective of the geometries involved.

While  $SbO_2$  and  $BiO_2$  geometries are not available, the Sb–O and Bi–O bond lengths are expected to be significantly greater than the P–O bond length as Sb and Bi are much larger atoms. The bond lengths of PO, SbO, and BiO are 1.476, 1.826, and 1.934  $\text{\AA}$ , respectively.<sup>34</sup> The dioxides of Sb and Bi might be too large to lead to dioxides within a single step. Any transition state potentially leading to the dioxide product might simply be too far from the equilibrium of ground state  $O_3$  and too far from the equilibrium of excited states of the dioxide products to allow access at low collision energy. This geometry change is consistent with the high-energy barrier associated with the earlier peak in time-dependent spectra of both Bi atom and  $Sb_n + O_3$  reactions.

Possibly more important than geometric considerations of electronic states is the role of ionic surfaces in the mechanisms for some of the CL pathways observed. Specifically, the question of whether a harpooning mechanism may be active for Sb and Bi forming monoxides, in addition to any other possible mechanisms, which might lead to dioxides. One might expect the harpoon mechanism to be unimportant for the P reactions because of a much shorter distance at which an electron jump would occur. An electron jump from M to  $O_3$  yielding an  $O_3^-$  that would dissociate most favorably to  $O_2 + O^-$ .<sup>50</sup> The  $O_2$  molecule would be very stable and the  $O^-$  would be much more likely to react, and thus form  $MO^*$ . In the absence of any harpooning mechanism, the formation of  $PO_2^*$  would then be preferred over the formation of  $PO^*$  from ions. In fact, the harpooning distance for P is much less than for Sb and Bi, 1.72 vs 2.20 and 2.78  $\text{\AA}$ , respectively. These distances were calculated from ionization potentials of

the group VA elements and the electron affinity of  $O_3$  obtained from the CRC Handbook.<sup>51</sup> The fact that they increase in going down group VA is consistent with decreasing barriers for reaching a crossing to an ionic surface leading to  $MO^*$ , as suggested by our analysis of the fast peaks in the time-dependent spectra for Sb and Bi. Thus the barrier to reaction (1), for M=P, is likely to be prohibitively high, and a likely reason for our failure to observe  $PO^*$  CL. For a complete description of the harpooning mechanism, see Menzinger's review.<sup>52</sup>

The differences between Bi and Sb are somewhat puzzling. Bi atoms apparently undergo a second-order process with respect to  $O_3$  to form  $BiO_2$ , but in the case of  $Sb_n$ , it is the dimers that appear to undergo a second-order process with respect to  $O_3$  to form  $SbO_2$ . It is possible that in each case there might be another reaction channel that was not observed because its signal was swamped by the major process.

This system of reactions does call for further investigation since the experimental conditions in some of the experiments were less than ideal to gain a complete understanding of all the processes involved. The time-dependent experiments should be extended to higher collision energies to characterize the early peaks of the Sb and Bi reactions. The dispersed-CL spectra for Sb and Bi reactions should be studied at a larger range of  $O_3$  pressures to determine the onset of the two-step mechanism, as exhibited by second-order dependences in  $O_3$ . Also, an investigation into reactions of these reactants leading to ground state products, possibly via laser-induced fluorescence, would be informative.

## CONCLUSIONS

The reactions of P, Sb, and Bi atoms and dimers with  $O_3$  lead to excited monoxides and dioxides under different conditions and apparently through different mechanisms. Phosphorus atoms react via (2). No  $PO^*$  products were observed. Two-step mechanisms were not observed for P atoms or dimers. Antimony atoms were observed to react via (1) and possibly through (2). Antimony dimers were observed to react via the mechanisms (5)+(3) or (7)+(10). Antimony atoms may also react via (1)+(3), although the presence of this mechanism is uncertain. Bismuth atoms appeared to react through (1), but not (2), and through the two-step mechanism (1)+(3). Bismuth dimers were not observed to react.

The P+ $O_3$  time dependence indicated a barrierless, attractive reaction cross section to form  $PO_2^*$ , while Sb and Bi atom reactions with  $O_3$  required very high collision energies (roughly 50 and 40  $\text{kJ mol}^{-1}$ , respectively), in order to form excited state  $MO^*$  products. Reactions observed to be second order in  $O_3$  for  $Sb_n$  and Bi atoms showed no barrier to reaction.

## ACKNOWLEDGMENTS

We would like to thank the National Science Foundation for its support of this research and Michael Oberlander for his assistance with some experiments.

- <sup>1</sup>G. Herzberg, *Molecular Spectra and Molecular Structure: III. Electronic Spectra and Electronic Structure of Polyatomic Molecules* (Van Nostrand Reinhold, New York, 1966).
- <sup>2</sup>D. K. Hsu, D. L. Monts, and R. N. Zare, *Spectral Atlas of Nitrogen Dioxide* (Academic, New York, 1978).
- <sup>3</sup>K. Uehara and H. Sasada, *High Resolution Spectral Atlas of Nitrogen Dioxide* (Springer-Verlag, New York, 1985), pp. 559–597.
- <sup>4</sup>A. E. Douglas and K. P. Huber, *Can. J. Phys.* **43**, 74 (1965).
- <sup>5</sup>J. L. Hardwick and J. C. D. Brand, *Chem. Phys. Lett.* **21**, 458 (1973).
- <sup>6</sup>J. L. Hardwick and J. C. D. Brand, *Can. J. Phys.* **54**, 80 (1976).
- <sup>7</sup>A. J. Merer and K-E. J. Hallin, *Can. J. Phys.* **56**, 838 (1978).
- <sup>8</sup>W. J. Lafferty and R. L. Sams, *J. Mol. Spectrosc.* **66**, 478 (1977).
- <sup>9</sup>A. Weaver, R. B. Metz, S. E. Bradforth, and D. M. Neumark, *J. Chem. Phys.* **90**, 2070 (1989).
- <sup>10</sup>A. Delon and R. Jost, *J. Chem. Phys.* **95**, 5686 (1991).
- <sup>11</sup>R. Georges, A. Delon, and R. Jost, *J. Chem. Phys.* **103**, 1732 (1995).
- <sup>12</sup>Y. Morino, M. Tanimoto, S. Saito, E. Hirota, R. Awata, and T. Tanaka, *J. Mol. Spectrosc.* **98**, 331 (1983).
- <sup>13</sup>G. D. Gillispie, A. U. Khan, A. C. Wahl, R. P. Hosteny, and M. Krausa, *J. Chem. Phys.* **63**, 3425 (1975).
- <sup>14</sup>C. F. Jackels and E. R. Davidson, *J. Chem. Phys.* **64**, 2908 (1976).
- <sup>15</sup>C. F. Jackels and E. R. Davidson, *J. Chem. Phys.* **65**, 2941 (1976).
- <sup>16</sup>G. Hirsch and R. J. Buenker, *Can. J. Chem.* **63**, 1542 (1985).
- <sup>17</sup>G. Hirsch, R. J. Buenker, and C. Petrongolo, *Mol. Phys.* **70**, 835 (1990).
- <sup>18</sup>M. Krauss, R. J. Celotta, S. R. Mielczarek, and C. E. Kuyatt, *Chem. Phys. Lett.* **27**, 285 (1974).
- <sup>19</sup>H. Köppel, W. Domcke, and L. S. Cedarbaum, *Adv. Chem. Phys.* **57**, 59 (1984).
- <sup>20</sup>R. Verma and C. McCarthy, *Can. J. Phys.* **61**, 11 849 (1983).
- <sup>21</sup>K. Kawaguchi, S. Saito, E. Hirota, and N. Ohashi, *J. Chem. Phys.* **82**, 4893 (1985).
- <sup>22</sup>P. A. Hamilton and T. P. Murrells, *J. Phys. Chem.* **90**, 182 (1986).
- <sup>23</sup>P. A. Hamilton, *J. Chem. Phys.* **86**, 33 (1987).
- <sup>24</sup>M. E. Fraser and D. H. Stedman, *J. Chem. Soc., Faraday Trans. 1* **79**, 527 (1983).
- <sup>25</sup>M. E. Fraser, D. H. Stedman, and T. M. Dunn, *J. Chem. Soc., Faraday Trans. 1* **80**, 285 (1984).
- <sup>26</sup>D. Harris, M. Chou, and T. Cool, *J. Chem. Phys.* **82**, 3502 (1985).
- <sup>27</sup>L. L. Lohr, *J. Phys. Chem.* **88**, 5569 (1984).
- <sup>28</sup>Z.-L. Cai, G. Hirsch, and R. J. Buenker, *Chem. Phys. Lett.* **255**, 350 (1996).
- <sup>29</sup>Y. Kabbadj and J. Lievin, *Phys. Scr.* **40**, 259 (1989).
- <sup>30</sup>R. Withnall, M. McCluskey, and L. Andrews, *J. Phys. Chem.* **93**, 126 (1989).
- <sup>31</sup>Z. Mielke, M. McCluskey, and L. Andrews, *Chem. Phys. Lett.* **165**, 146 (1990).
- <sup>32</sup>L. Andrews, M. McCluskey, Z. Mielke, and R. Withnall, *J. Mol. Struct.* **222**, 95 (1990).
- <sup>33</sup>M. McCluskey and L. Andrews, *J. Phys. Chem.* **95**, 2988 (1991).
- <sup>34</sup>K. P. Huber and G. Herzberg, *Molecular Spectra and Molecular Structure IV: Constants of Diatomic Molecules* (Van Nostrand Reinhold, New York, 1979).
- <sup>35</sup>M. W. Chase, Jr., C. A. Davis, J. R. Downey, Jr., D. J. Frurip, R. A. McDonald, and A. N. Syverud, *J. Phys. Chem. Ref. Data Suppl.* **14**, 1 (1985).
- <sup>36</sup>A. Twarowski, *Combust. Flame* **94**, 91 (1993).
- <sup>37</sup>A. J. A. Aquino and P. R. Taylor, *Chem. Phys. Lett.* **249**, 130 (1996); J. Drowart, C. E. Myers, R. Szwarc, A. VanderAuwera-Mahieu, and O. M. Uy, *J. Chem. Soc., Faraday Trans. 2* **68**, 1749 (1972); S. A. Jarrett-Sprague, I. H. Hillier, and I. R. Gould, *Chem. Phys.* **140**, 27 (1990).
- <sup>38</sup>B. S. Cheong, M. D. Oberlander, R. P. Kampf, and J. M. Parson, *J. Chem. Phys.* **99**, 5104 (1993).
- <sup>39</sup>W. J. Rosano and J. M. Parson, *J. Chem. Phys.* **84**, 6261 (1986).
- <sup>40</sup>J. M. Parson, L. C. Geiger, and T. J. Conway, *J. Chem. Phys.* **74**, 5595 (1981).
- <sup>41</sup>Equilibrium mole fractions were calculated based upon a fixed total vapor pressure and from thermodynamic values from R. Hultgren, P. D. Desai, D. T. Hawkins, M. Gleiser, K. K. Kelly, and D. D. Wagman, *Selected Values of the Thermodynamic Properties of the Elements* (American Society for Metals, Metals Park, OH, 1973).
- <sup>42</sup>A. Gonzalez Ureña, *Mol. Phys.* **52**, 1145 (1984).
- <sup>43</sup>A. Gonzalez Ureña, in *Advances in Chemical Physics*, edited by I. Prigogine and S. A. Rice (Wiley, New York, 1987), Vol. LXXVI.
- <sup>44</sup>D. M. Manos and J. M. Parson, *J. Chem. Phys.* **63**, 3575 (1975).
- <sup>45</sup>J. E. Velazco and D. W. Setser, *J. Chem. Phys.* **62**, 1990 (1975).
- <sup>46</sup>R. C. Oldenborg, J. L. Gole, and R. N. Zare, *J. Chem. Phys.* **60**, 4032 (1974).
- <sup>47</sup>M. D. Oberlander and J. M. Parson, *J. Chem. Phys.* **97**, 150 (1992).
- <sup>48</sup>E. Rosen, *Tables Internationales de Constantes Sélectionnées, Données Spectroscopiques Relatives aux Molécules Diatomiques* (Pergamon, New York, 1970), Vol. 17.
- <sup>49</sup>W. L. Jorgensen and L. Salem, *The Organic Chemist's Book of Orbitals* (Academic, New York, 1973).
- <sup>50</sup>M. H. Covinsky, A. G. Suits, H. F. Davis, and Y. T. Lee, *J. Chem. Phys.* **97**, 2515 (1992).
- <sup>51</sup>*CRC Handbook of Chemistry & Physics*, 77th ed., edited by D. R. Lide (CRC Press, New York, 1996).
- <sup>52</sup>M. Menzinger, in *Gas Phase Chemiluminescence and Chemiionization*, edited by A. Fontijn (North Holland, Amsterdam, 1985).